Journal of Materials Chemistry B

ROYAL SOCIETY OF CHEMISTRY

PAPER

View Article Online
View Journal | View Issue

Cite this: J. Mater. Chem. B, 2022, 10, 2691

Antibacterial thyme oil-loaded zwitterionic emulsion hydrogels†

Gangchen Lu,‡[ab] Xin Shen,‡[ab] Dongdong Xiao,[c] Liduo Rong,[ab] Zhiping Mao,[abd] Bijia Wang,[a] Xiaofeng Sui,*[ab] Meixin Zhao*[e] and Xueling Feng *[abd]

Emulsion hydrogels are structurally composite materials combining the advantages of emulsions and hydrogels with the ability to accommodate hydrophobic and hydrophilic components in one system. It is a promising strategy for the excellent encapsulation and delivery of many bioactive ingredients. In this work, the thyme oil-loaded zwitterionic emulsion hydrogels are constructed by the cellulose acetoacetate-horseradish peroxidase-hydrogen peroxide-initiated (CAA-HRP-H_2O_2-initiated) ternary enzyme-mediated polymerization of the thyme oil-in-water (O/W) emulsions stabilized by cellulose acetoacetate (CAA). CAA is the key component in the system, acting as the emulsifier and the polymerization mediator simultaneously. The formed zwitterionic poly(sulfobetaine methacrylate) (PSBMA) hydrogel network provides emulsion hydrogels with good hydration capacity and potential anti-fouling performance. The thyme oil-loaded zwitterionic emulsion hydrogels exhibit interconnected, uniform, and adjustable porous structures with tunable mechanical properties, antifouling performance, good biocompatibility, and excellent antibacterial activity against *S. aureus* and *E. coli*. These results all demonstrate that the ternary enzyme-mediated polymerization of zwitterionic monomers in the continuous phase of O/W emulsion templates is a facile and efficient strategy to encapsulate hydrophobic bioactive ingredients.

Received 28th December 2021,
Accepted 20th January 2022

DOI: 10.1039/d1tb02853g

rsc.li/materials-b

Introduction

Currently, hydrophobic active ingredients, such as drugs, essential oils, fat-soluble vitamins, and fatty acids, are ubiquitous in the pharmaceutical, cosmetic, and food industries.[1,2] However, the inherent hydrophobicity and liquid form of those materials limit their bioavailability and hinder their usage in practical applications.[1] The oil-in-water (O/W) emulsion system has been widely pursued to stabilize, load, and deliver hydrophobic active ingredients.[3] The O/W emulsions are formed by dispersing the oil phase into the continuous aqueous phase through emulsification with amphiphilic surfactants. The O/W emulsion droplets could stabilize hydrophobic active components in the aqueous phase and protect them from oxidation, hydrolysis, and degradation.[4] The oil phase acted as a reservoir for dissolving hydrophobic drug molecules.[5] Moreover, the functional oil itself, such as plant essential oil, could be directly used as the oil phase that dispersed in the continuous aqueous phase.[6] For instance, Ahmed *et al.* investigated the encapsulation and release of curcumin, a natural bioactive ingredient, with the oil-in-water emulsion-based delivery system to enhance its solubility and bioavailability.[7] However, the thermodynamical instability of emulsion systems would induce the oil and water phases' reversion *via* coalescence, flocculation, and Ostwald ripening. The stability, functional characteristics, and release behavior of bioactive ingredients would be impaired. Therefore, improving the stability and effectiveness of emulsions is still challenging.

Hydrogels are constructed by the three-dimensional (3D) hydrophilic polymeric network in an aqueous environment.[8] Due to their intrinsic hydrophilicity, excellent biocompatibility, and tunable physicochemical and mechanical characteristics, hydrogels as encapsulation materials have attracted a great deal of attention. The hydrogel encapsulation strategy has been extensively employed in biomedical fields such as wound dressings, drug delivery carriers, and cell culture scaffolds.[1,5,6,9,10] For example, Zhu *et al.* prefabricated the chlorhexidine diacetate (CHX)-loaded nanogels (CLNs)

[a] Key Lab of Science and Technology of Eco-Textile, Ministry of Education, College of Chemistry, Chemical Engineering and Biotechnology, Donghua University, Shanghai 201620, People's Republic of China. E-mail: suixf@dhu.edu.cn, xlfeng@dhu.edu.cn
[b] National Engineering Research Center for Dyeing and Finishing of Textiles, Donghua University, Shanghai, 201620, People's Republic of China
[c] Department of Urology and Andrology, Ren Ji Hospital, Shanghai Jiao Tong University School of Medicine, Shanghai, 200127, People's Republic of China
[d] National Manufacturing Innovation Center of Advanced Dyeing and Finishing Technology, Tai'an, Shandong, 271000, People's Republic of China
[e] Department of Nuclear Medicine, Peking University Third Hospital, Beijing, 100191, People's Republic of China. E-mail: zhaomeixin.student@sina.com

† Electronic supplementary information (ESI) available. See DOI: 10.1039/d1tb02853g

‡ These authors contributed equally.

and incorporated the CLNs into hydrogel networks, which were synthesized by the photo-crosslinking of aminoethyl methacrylate hyaluronic acid (HA-AEMA) and methacrylated methoxy polyethylene glycol (mPEG-MA). The CLNs-loaded hybrid hydrogels possessed rapid hemostasis, sustainable drug release, and antibacterial properties, which could be utilized as excellent wound dressings.[9] Nonetheless, direct hydrogel encapsulation was restricted by the heterogeneity.

Emulsion hydrogel, which is a promising and desirable strategy to load and deliver bioactive components in biomedical applications, combines the uniformity of the emulsions and the biocompatibility of the hydrogels. On the one hand, the stability of O/W emulsions and the encapsulation efficiency of active ingredients could be substantially improved by the *in situ* polymerization of the hydrogel networks. On the other hand, the biphasic system is capable of accommodating both hydrophobic and hydrophilic components through a facile and versatile preparation process. Badruddoza *et al.* reported the core–shell composite hydrogels prepared by embedding polyvinyl alcohol-stabilized O/W emulsion in alginate hydrogels to encapsulate and release the lipophilic active pharmaceutical ingredient (fenofibrate). The strategy significantly improved the solubility, bioavailability, and loadings of fenofibrate.[11]

In spite of the advantages of the emulsion hydrogel, the previous reported approaches mainly focused on the building of the aqueous phase network with existing polymers, which meant the choice of materials might be limited. A few examples of emulsion hydrogels utilized *in situ* polymerization to build the aqueous phase network from monomers with normal polymerization strategy, which was inevitably related to the use of bio-unfriendly initiators. Currently, enzyme-mediated polymerization has attracted increasing attention in the preparation of biomedical materials due to its biocompatibility, mild reaction conditions, and environmental-friendliness.[12] Horseradish peroxidase (HRP) is an enzyme extracted from the root of horseradish, which primarily consists of heme, a compound of protoporphyrin and Fe(III).[13] The enzyme initiation system, which is comprised of HRP, the oxidant H_2O_2 and the polymerization mediator acetylacetone (ACAC) has been well investigated and utilized to initiate the polymerization of vinyl monomers to construct hydrogels.[14] Su *et al.* reported a convenient and mild approach to prepare the nanocomposite hydrogels *via* the HRP/H_2O_2/ACAC-initiated polymerization of the monomer *N*,*N*′-dimethylacrylamide. The prepared hydrogels exhibited excellent mechanical performance, stability, and enhanced enzymatic activity, and had great promise in biological applications.[15]

Using enzymatic polymerization, thyme-oil loaded zwitterionic emulsion hydrogels with advanced antibacterial and antifouling performance are designed and developed in this study. Thyme oil, a plant essential oil extracted from thyme leaves and flowers, having extensive applications in cosmetic and biomedical fields due to its natural favorable antibacterial and anti-inflammatory activities, was chosen as the dispersing phase.[16,17] The functional cellulose derivative, cellulose acetoacetate (CAA), was chosen as the emulsifier to stabilize the thyme oil-in-water emulsion for its amphiphilicity. Moreover, the acetoacetyl group on the CAA side chain was able to serve as the polymerization mediator, working effectively with HRP and H_2O_2 to initiate the *in situ* polymerization of zwitterionic monomers SBMA, and build the continuous aqueous phase network. Polyzwitterionic chains carrying both cationic and anionic groups would endow the emulsion hydrogel with strong hydration capacity *via* ionic solvation and excellent biocompatible, anti-fouling, and anti-inflammatory properties. While the zwitterionic hydrogels employed as wound dressings, biosensors, tissue fillers and drug delivery platforms have been profoundly investigated and extensively reported,[18–27] the zwitterionic emulsion hydrogels are seldom presented.

Herein, we demonstrate the successful fabrication of a zwitterionic hydrogel *via in situ* polymerization of the CAA stabilized O/W emulsion, employing a typical zwitterionic poly(sulfobetaine methacrylate) (PSBMA) to construct the aqueous phase network for the encapsulation of thyme oil. CAA played an important role in the system, acting as the emulsifier and the polymerization mediator simultaneously. The resultant thyme oil-loaded zwitterionic emulsion hydrogels possessed excellent antibacterial activity, biocompatibility, and antifouling capacity. The morphology and mechanical properties of the emulsion hydrogel were investigated in detail. The zwitterionic emulsion hydrogels would hold promise as a material for wound dressing.

Experimental section

Materials

[2-(Methacryloyloxy)ethyl]dimethyl-(3-sulfopropyl)ammonium hydroxide (SBMA), *N*,*N*′-methylenebisacrylamide (MBA), horseradish peroxidase (HRP, EC 1.11.1.7, M_W = 40 kDa, 300 U mg^{-1}) and phosphate-buffered saline (PBS, pH = 7.4) were purchased from Aladdin Reagent Co., Ltd. (Shanghai, China). Hydrogen peroxide (H_2O_2, 30 wt%) and *tert*-butyl acetoacetate (*t*-BAA, 99%) were obtained from Sinopharm Chemical Reagent Co., Ltd. The wood pulp was supplied by Xinxiang Natural Chemical Co., Ltd. The ionic liquid 1-allyl-3-methylimidazolium chloride (AMIMCl) was purchased from the Center for Green Chemistry and Catalysis (CGCC), LICP, CAS. The thyme oil (thymol content $\geq$ 30.0%) was purchased from Jiangxi Xuesong Natural Medicinal Oil Co., Ltd. All chemicals were analytical grade and used without further purification.

Synthesis of cellulose acetoacetate (CAA)

Cellulose acetoacetate (CAA) was synthesized according to a previously reported method.[28] Briefly, the wood pulp was crushed into cellulose powder. The cellulose powder (1.0 g) was evenly dispersed in 1-allyl-3-methylimidazolium chloride (AMIMCl) (24.0 g). The mixture was stirred at 90 °C until it was completely dissolved. Dimethylformamide (DMF) (19.6 mL) was added and the transparent cellulose solution was obtained. Afterwards, the solution was heated to 110 °C and *tert*-butyl acetoacetate (*t*-BAA, 3.4 g) was added dropwise, then keep stirring for another 2 hours. Finally, the products were

precipitated and washed by ethanol several times and dried at 60 °C in a vacuum for 12 hours.

Preparation of thyme oil-loaded emulsions

To 1.4 mL of 2 wt% CAA aqueous solution, 0.6 g of SBMA and 6 mg of MBA were added. The mixture served as the continuous phase. The thyme oil (0.35 mL, 0.934 mL) acting as the dispersed phase was added to the aqueous phase. The mixture was ultrasonicated with an ultrasonic cell pulverizer (SCIENTZ, JY92-IIDN, China) at a frequency of 20 kHz with a power of 240 W for 2 minutes to form the oil-in-water emulsion.

Preparation of emulsion hydrogels

50 μL of HRP solution (8 mg mL^{-1}) and 4 μL of 30% H_2O_2 solution were added sequentially into the aforementioned O/W emulsions with the internal oil phase volume fraction of 20% and 40%. The correponding emulsion hydrogels (H-20%, H-40%) were then synthesized by CAA-HRP-H_2O_2 enzyme-initiated radical polymerization at ambient temperature (25 °C) for 30 minutes. As a control, HRP solution (50 μL, 8 mg mL^{-1}) and 30% H_2O_2 solution (4 μL) were added to the aqueous phase consisting of 2 wt% CAA aqueous solution (1.4 mL) with SBMA (0.6 g) and MBA (6 mg) at 25 °C for 30 minutes to obtain the hydrogel (H-0%). The specific experimental composition parameters of emulsion hydrogels have been shown in Table S1 (ESI†).

Morphology of emulsions

The emulsion samples were diluted with deionized water. The emulsion droplets were observed using an optical microscope (ECLIPSE 80i, NIKON, Japan) at room temperature. And the size distribution of emulsion droplets was calculated by the ImageJ software.

Morphology of emulsion hydrogels

The emulsion hydrogels were immersed in deionized water for 24 hours to remove impurities and then freeze-dried for 24 hours. The microstructure of samples was characterized by a scanning electron microscope (TM-3030, Hitachi, Japan) at an accelerating voltage of 5 kV after gold coating.

FTIR spectra

Fourier transform infrared (FTIR) spectroscopy was analyzed on a PerkinElmer Spectrum Two (USA) equipped with an attenuated total reflectance (ATR) accessory in the spectra from 4000 to 400 cm^{-1} with a resolution of 4 cm^{-1}.

Compressive mechanical tests

The samples were prepared in a cylindrical shape (18 mm in diameter and 6 mm thick). The compressive stress–strain property was measured on a universal testing machine (HY 940F, China) with a strain from 0% to 60% at a compression rate of 2 mm min^{-1}. The modulus was calculated from the linear portion of the stress–strain curve.

Rheology tests

Rheological analyses of the samples were performed utilizing a Thermo HAAKEMARS 60 rheometer (Thermo, USA). The cylinder-shaped samples (18 mm in diameter and 3 mm thick) were set under a 25 mm diameter parallel plate with a gap of 3 mm. The oscillatory frequency sweep was operated in an oscillatory frequency range (ω) of 1–100 rad s^{-1} at a constant shear strain (γ) of 1% at 25 °C. The oscillatory strain sweep was operated in an oscillatory strain range (γ) of 1%–100% at a constant frequency (ω) of 1 rad s^{-1} at 25 °C.

Equilibrium water content (EWC) measurements

The EWC of H-0%, H-20% and H-40% was assessed by weighing the mass of fully hydrated and dry samples. First, the hydrogels and emulsion hydrogels were separately immersed in deionized water for two days at 25 °C for complete swelling. The fully wet and swollen samples were then weighed, denoted as W_w. The wet samples were freeze-dried for 24 hours and reweighed, denoted as W_d. The EWC of the samples was calculated as follows:[30]

$$\mathrm{EWC}(\%) = \frac{W_w - W_d}{W_d} \times 100\%$$

Determination of release capacity

The main component of thyme oil was thymol. And the signal of thymol in absorbance could be determined with a UV–VIS spectrophotometer (UV-1800, SHIMAZDU, Japan). Thus, the emulsion hydrogels were placed in 100 mL of PBS solution (pH 7.4) to release the thyme oil in a closed glass flask for 1, 2, 4, 8, 12, 24, 48, 72, and 96 hours, respectively. Before each measurement of absorbance, 2 mL of the solution were removed and diluted 10 times. And then, 2 mL of PBS solution was added to the original solution, which guaranteed the same amount of solution. The concentrations of thyme oil were calculated using the calibration curve obtained in a range of 0.005–0.100 μL mL^{-1} of thyme oil (absorbance, at 274 nm, R^2 = 0.999).

Anti-fouling tests

Bovine serum albumin (BSA) was used as a model organic foulant in this study. The adsorption propensities were characterized by measuring the fluorescence intensity of the hydrogel surfaces after being exposed to the BSA-FITC solution (0.05 mg mL^{-1}) for 1 h and 3 h, respectively. The BSA-FITC adsorbed samples were captured using an epifluorescence optical microscope (ECLIPSE 80i, NIKON, Japan) with a filter at 495/520 nm.

Evaluation of the antibacterial property

The antibacterial activity of emulsion hydrogels (H-20%, H-40%) and hydrogels (H-0%) was evaluated by agar plate diffusion tests. Gram-negative model bacteria (*E. coli*) and Gram-positive model bacteria (*S. aureus*) were chosen as model

strains.[9] The bacterial suspension (0.1 mL) was spread on the fresh nutrient agar plate. Then the sample piece (18 mm in diameter and 2 mm in height) was placed on the nutrient agar surface. The agar plate inoculated with bacteria was incubated at 37 °C for 24 hours. The antibacterial property of emulsion hydrogels was intuitively evaluated by the appearance of the zone of inhibition (ZOI). The specific antibacterial capacity was further assessed by the numerical value of ZOI, which was defined as follows:

$$\mathrm{ZOI} = \frac{D - d}{2}$$

where D and d are the diameters of the inhibition and emulsion hydrogel, respectively.

Cell experiments

A Cell Counting Kit-8 (CCK-8) (Dojindo Laboratories, Kumamoto, Japan) was used to evaluate the biocompatibility according to the manufacturer's instructions. Briefly, H-0%, H-20%, and H-40% were sterilized by 70% ethanol and washed twice with distilled water. Then they were immersed in PBS solution at 37 °C for 24 hours under continuous stirring to extract related conditioned media. Human fibroblasts (purchased from the cell bank of Chinese Academy of Science, Shanghai, China) were seeded in a 96-well plate at 3000 cells per well and incubated overnight at 37 °C in humidified CO_2. Next, they were incubated in four groups with serum-free Dulbecco's modification of Eagle's medium (Thermo Fisher Scientific Inc., MA, USA) and related conditioned media, respectively. At each time point, 10 μL of CCK-8 reagent was added to each well and incubated for 4 hours at 37 °C in humidified CO_2, after which the absorbance at 450 nm was measured using a microplate reader (MULTISKAN MK3, Thermo Fisher Scientific Inc., MA, USA).

Results and discussion

Fabrication and characterization

As shown in Fig. 1a, the zwitterionic hydrogel was prepared by CAA-HRP-H_2O_2-initiated polymerization of the CAA aqueous solution containing the monomer SBMA and crosslinker MBA. The opalescent thyme oil-loaded zwitterionic emulsion hydrogels were synthesized by CAA-HRP-H_2O_2-initiated *in situ* polymerization of the CAA-stabilized O/W emulsions (Fig. 1b). The thyme oil, acting as the dispersed phase, was added into the CAA aqueous solution consisting of SBMA and MBA. Then the thyme oil-loaded emulsions were formed by ultrasonication. Ultimately, HRP and H_2O_2 were sequentially added to the O/W emulsions. By CAA-HRP-H_2O_2-initiated polymerization, the opalescent thyme oil-loaded zwitterionic emulsion hydrogels were successfully synthesized. CAA played an important role in the system, which could serve as a polymerization mediator and an emulsifier simultaneously. The former was attributed to the β-diketone structure of the acetoacetate group, the latter was due to its amphiphilic properties. The formation of the zwitterionic hydrogel and zwitterionic emulsion hydrogel

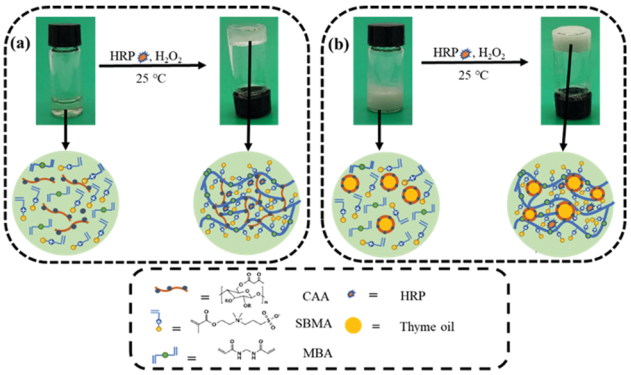

Fig. 1 Schematic illustration of the fabrication procedure of (a) the hydrogel and (b) the emulsion hydrogel *via* CAA-HRP-H_2O_2 ternary enzyme-mediated radical polymerization.

was further verified by a vial inversion test, as displayed in Fig. 1a and b.

The chemical structure of CAA was analyzed by the FTIR spectra shown in Fig. 2a. Compared with cellulose, the CAA has distinct characteristic peaks emerging at 1706 and 1737 cm^{-1} that correspond to the stretching vibration of the ketone carbonyl (O═C–CH_3) and ester carbonyl (O═C–O), respectively. The presence of these peaks confirms the successful modification of cellulose with the acetoacetate functional group by transesterification of cellulose with *tert*-butyl acetoacetate.[28] The ^{1}H NMR spectra of CAA also indicates the successful modification of the acetoacetate group on the cellulose backbones (Fig. S1, ESI†). By calculation, the substitution degree of the acetoacetate group in cellulose is about 0.78.

In consideration of the interference of thyme oil compounds on the chemical composition of the gel system, we selected the lyophilized hydrogel H-0% without thyme oil as the standard sample. The FTIR spectra of the zwitterionic monomer SBMA and the hydrogel H-0% are displayed in Fig. 2b. In the hydrogel H-0%, the characteristic absorption band at 3100–3680 cm^{-1} is assigned to the stretching vibration of associated hydroxyl peaks. The characteristic peaks at 1722 cm^{-1} and 1477 cm^{-1} are attributed to the O═C–O stretching vibration and the –$N^+(CH_3)_2$– in-plane bending vibration, respectively. The absorption band at 1080–1260 cm^{-1} corresponds to the C–N stretching vibration. The characteristic peaks at 1036 and 1169 cm^{-1} belong to the symmetric and asymmetric stretching vibrations of S═O. The peak at 602 cm^{-1} is ascribed to the

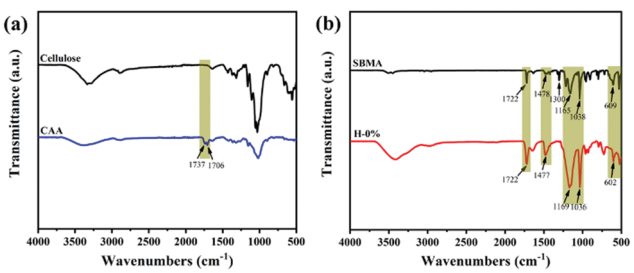

Fig. 2 FT-IR spectra of (a) cellulose and CAA, (b) SBMA and H-0%.

stretching vibration of C–S. The presence of a series of primary characteristic peaks of SBMA, and the absence of the characteristic peak at 1300 cm^{-1} (referred to the in-plane deformation vibration of $C{=}CH_2$), both reveal that the zwitterionic monomer SBMA was successfully polymerized by the CAA-HRP-H_2O_2 ternary initiation system. The content of CAA in the gel system is so low that the characteristic peaks of CAA are absent in the infrared spectra of H-0% hydrogel.

Morphology characterization

The digital photographs of O/W emulsions with the thyme oil phase fraction of 20% and 40% exhibited in Fig. 3a indicate that the prepared emulsions are sticky and milk-white. The corresponding morphology of emulsions observed by the optical microscope and the size distribution of emulsion droplets calculated by the ImageJ software are both displayed in Fig. 3b and c. And the diluted version of Fig. 3b and c is shown in Fig. S2 (ESI†). When the internal phase fraction is 20%, the emulsion droplets have a well-defined spherical shape and the particles are distributed uniformly with a size of approximately 1 μm. The amphiphilic CAA molecules are capable of stabilizing the thyme oil-loaded emulsions and inhibiting droplets aggregation and flocculation. With the thyme oil phase fraction increasing to 40%, the size of emulsion droplets increases and the distribution uniformity decreases slightly. The phenomenon can be ascribed to the deficiency of the concentration-invariant CAA in stabilizing the increased interfacial area resulting from the increased oil phase fraction.[6] The thyme oil-loaded emulsions are relatively stable. Even after storing for one week, there is no delamination of the emulsions in the vial. And the micromorphology and particle size distribution of the O/W emulsion droplets do not significantly vary (Fig. S3, ESI†), which further indicates that CAA molecules possess good emulsifying capability and the O/W emulsion system is able to stabilize and encapsulate thyme oil.

It is well known that the 3D porous structure of hydrogels as wound dressings can provide gas exchange channels for improving wound healing.[29] Therefore, the macrostructure of the emulsion hydrogels is of great interest. As revealed in SEM images, the microstructures of the freeze-dried hydrogel H-0% (Fig. 4a) are irregular and macroporous. The pore structures of the freeze-dried emulsion hydrogels H-20% (Fig. 4b) and H-40% (Fig. 4c) prepared by *in situ* polymerization of O/W emulsions are interconnected, regular, and uniform. In addition, their pore sizes (1 μm–3 μm) are smaller than those of hydrogel H-0% (about 5 μm). The pore sizes of the emulsion hydrogels correspond to the respective emulsion droplets. It is observed that the increase of the thyme oil phase fraction results in the enhancement of the pore diameter and the thinning of the pore wall of emulsion hydrogels.

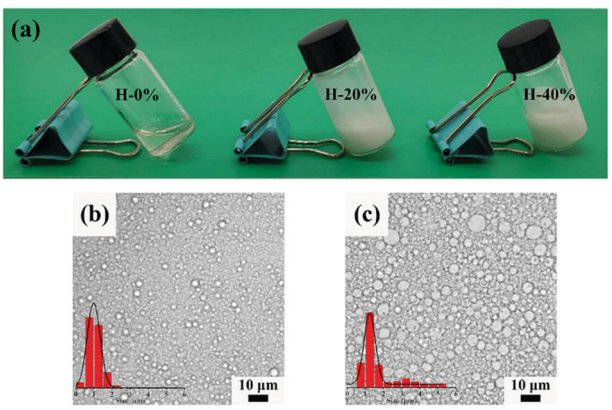

Fig. 3 Digital photographs (a) and optical micrographs of the fresh O/W emulsions with the thyme oil phase fraction of (b) 20% and (c) 40%.

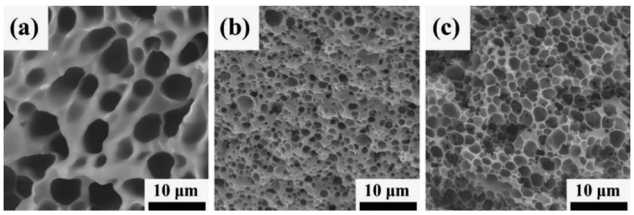

Fig. 4 SEM images of the freeze-dried hydrogel and emulsion hydrogels. (a) H-0%, (b) H-20%, and (c) H-40%.

Mechanical properties

The mechanical properties of emulsion hydrogels were analyzed by compression and rheology tests. The compressive stress–strain curves in Fig. 5a indicate that all the hydrogels H-0% and the emulsion hydrogels H-20% and H-40% can withstand a compressive strain of 60% and then well recover to their original shape after removing the compression force because of the elasticity of the zwitterionic hydrogel network. At a compressive strain of 60%, the compressive stress values of H-0%, H-20%, and H-40% are 113.5 kPa, 91.5 kPa, and 77.8 kPa, respectively. The corresponding compressive modulus values are 97.0 kPa, 79.5 kPa, and 59.2 kPa, respectively (Fig. 5b). The reduction of compressive stress and modulus is

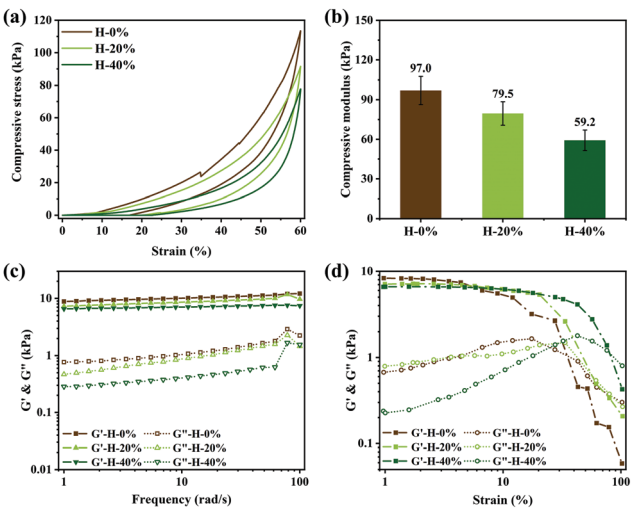

Fig. 5 (a) Compressive stress–strain curves and (b) modulus of H-0%, H-20%, and H-40%. Rheological behavior of H-0%, H-20%, and H-40% during (c) oscillatory frequency sweep and (d) oscillatory strain sweep.

due to the decrease in the relative content of polymer networks in emulsion hydrogels resulting from the incorporation of thyme oil. It is worth mentioning that under cyclic compressive stress–strain tests, the hydrogel H-0% is easy to be crushed, while the mechanical properties of the emulsion hydrogels do not change (Fig. S4, ESI†). These results indicate that the emulsion hydrogels have good elasticity and shape-recovery capacity because of the addition of thyme oil. To investigate the stability of the emulsion hydrogels after releasing the thyme oil, the emulsion hydrogels were placed in the PBS solution for 48 hours and their mechanical behavior was tested again. It is interesting that the mechanical properties of the swelling emulsion hydrogels are improved to some extent, which is attributed to the increased energy dissipation capacity of the entire hydrogel network due to water absorption (Fig. S5, ESI†).

The rheological behaviors of emulsion hydrogels in the oscillatory frequency sweep are displayed in Fig. 5c. The storage modulus (G') is higher than the loss modulus (G'') of the gel materials, which further demonstrates that the gel networks have outstanding elasticity. The G' and G'' of the H-0%, H-20% and H-40% exhibit a slightly decreasing trend with the increase of thyme oil. Even if the thyme oil phase fraction is up to 40%, the G' of the emulsion hydrogel can reach up to 6 kPa. In the oscillatory strain sweep depicted in Fig. 5d, the storage modulus G' of samples is basically stable in the low strain range. When the strains exceed their respective critical strain values, G' reduces dramatically, which can be owing to the collapse of the hydrogel's 3D network structure. The emulsion hydrogels H-20% and H-40% loaded with thyme oil can sustain substantially greater strain ranges than hydrogel H-0%, which is attributable to the fact that thyme oil effectively dissipates energy and weakens stress concentration. In addition, we find that there is no positive correlation between the amount of SBMA and the samples' strength. As shown in Fig. S6 (ESI†), the G' of the emulsion hydrogel reaches the maximum when the amount of SBMA is medium. It can be explained as the negative effect of SBMA on emulsion stability. Owing to its high charge, SBMA damages the emulsifying ability of CAA and the larger emulsion droplets will be formed (Fig. S7, ESI†). Thermodynamically unstable emulsions have a considerable impact on subsequent polymerization, and the strength of the emulsion hydrogel is finally compromised. All the above results demonstrate that the zwitterionic emulsion hydrogels have excellent and adjustable mechanical properties.

Hydration property

The hydration property of the emulsion hydrogel has been examined. The wound dressing material with excellent water absorption capacity can provide a moist environment and uptake excess exudates to promote wound healing.[30] As shown in Fig. 6, the hydration property of the emulsion hydrogels is characterized by the equilibrium water content (EWC). The hydrogel H-0% has a high EWC of 192%, which is attributed to the dense hydration layer formed by electrostatic interaction of the zwitterionic PSBMA chains in the hydrogel network. While the thyme oil is incorporated into the emulsion

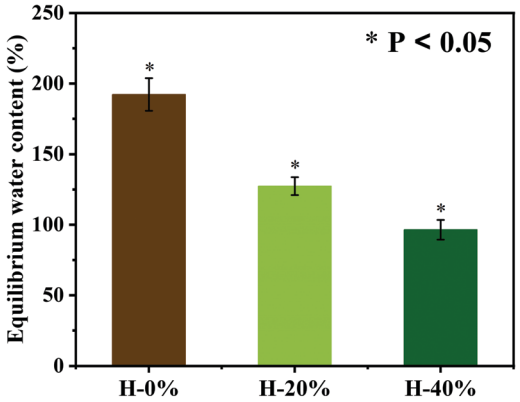

Fig. 6 Equilibrium water content (EWC) of H-0%, H-20%, and H-40%.

hydrogels, the hydrophobicity of the thyme oil wrapped in the hydrogel network would weaken the hydration capacity. The EWC of the emulsion hydrogels H-20% and H-40% are reduced slightly to 127% and 96%, respectively. The thyme oil-loaded emulsion hydrogels still maintain good hydration performance due to the strong affinity of zwitterionic PSBMA for water molecules.

Release behavior

Because of the barrier of the hydrogel network, the thyme oil in the emulsion hydrogels is released slowly. The detailed release curves are shown in Fig. 7a. Thyme oil was released quickly in the first 24 hours, but the rate diminished as time passed. After 24 hours, the release rate of thyme oil shows an approximate linear relationship with time. The maximum thyme oil release concentration was achieved at 72 hours and remained essentially constant thereafter. And even after 96 hours, the concentration of thyme oil is 0.42 μL mL^{-1} (H-40%) and 0.34 μL mL^{-1} (H-20%) (Fig. 7b), which further demonstrates the slow-release effect of emulsion hydrogels. In addition, the emulsion hydrogel H-40% released more thyme oil than the sample H-20% in the same time interval, indicating that the release rate of thyme oil in emulsion hydrogel can be controlled by adjusting the content of the inner phase.

Anti-fouling property

By evaluating the protein adsorption propensity onto the surfaces of the hydrogels, the anti-fouling behavior of the

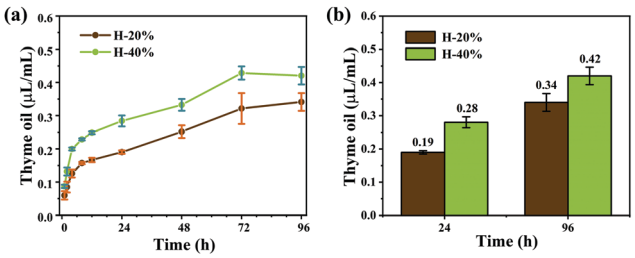

Fig. 7 (a) Release curves of thyme oil in emulsion hydrogels H-20% and H-40%, and (b) corresponding release data.

zwitterionic hydrogel H-0%, emulsion hydrogels H-20%, and PAM hydrogel was investigated. A labeled protein, BSA-FITC, was used to quantitatively compare the amounts of adsorbed protein among the hydrogel surfaces. Due to the fluorescence signal from the FITC dye in BSA-FITC, fluorescence microscopy images of protein-adsorbed hydrogels could be captured. As clearly revealed in Fig. 8, the fluorescence intensity on the zwitterionic hydrogel H-0% surface is much weaker than that on the PAM hydrogel surface. The statistical results are shown in Fig. S8 (ESI†). The enhanced anti-fouling effect of the zwitterionic hydrogels is due to the strong repulsive force between the polymer and BSA. With the thyme oil loaded, the fluorescence intensity of the emulsion hydrogel H-20% is slightly higher than that of the hydrogel H-0%, but still lower than that of the PAM hydrogel. Nevertheless, the thyme oil-loaded zwitterionic emulsion hydrogels still exhibit superior anti-fouling ability than normal hydrogels, which would be useful in the development of wound dressing materials.

Antibacterial activity

The antibacterial activities of the thyme oil-loaded zwitterionic emulsion hydrogels H-20% and H-40% against *S. aureus* and *E. coli* were assessed by the agar diffusion plate method. The hydrogel H-0% without thyme oil was served as a control. As shown in Fig. 9, there are no observable inhibition zones against *S. aureus* and *E. coli* for the hydrogel H-0%, indicating that it has no antibacterial activity. However, the emulsion hydrogels H-20% and H-40% produced distinct inhibition zones against *S. aureus* and *E. coli*. In addition, the ZOI value increases as the thyme oil phase fraction increases from 20% to 40%. To be specific, the ZOI value of the emulsion hydrogel H-20% and H-40% against *S. aureus* is 10.2 mm and 12.2 mm and against *E. coli* is 9.1 mm and 11.7 mm, respectively. The specific calculation process is displayed in Fig. S9 (ESI†). These results demonstrate that the thyme oil-loaded zwitterionic emulsion hydrogels possess outstanding antibacterial properties. The prepared zwitterionic thyme oil-loaded emulsion hydrogels are expected to be the promising materials as antibacterial wound dressings in biomedical fields.

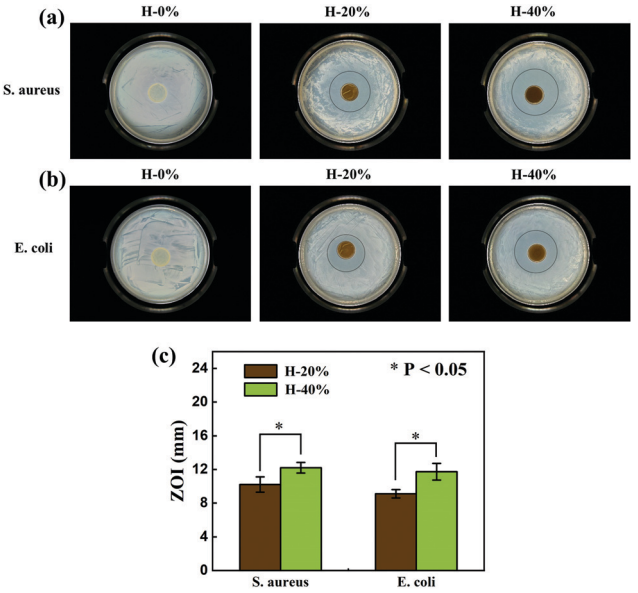

Fig. 9 Antibacterial activity of emulsion hydrogels against (a) *S. aureus* and (b) *E. coli*, (c) the corresponding average ZOI values of H-20% and H-40%.

Cyto-compatibility

Wound dressing materials should be cyto-compatible. A CCK-8 experiment was provided to examine the cell compatibility of the emulsion hydrogels. The results are exhibited in Fig. 10 which reveals that there is no significant difference in cell proliferation between samples and the blank control at each time point. These results collectively illustrate that the emulsion hydrogels are non-toxic and would not inhibit cell

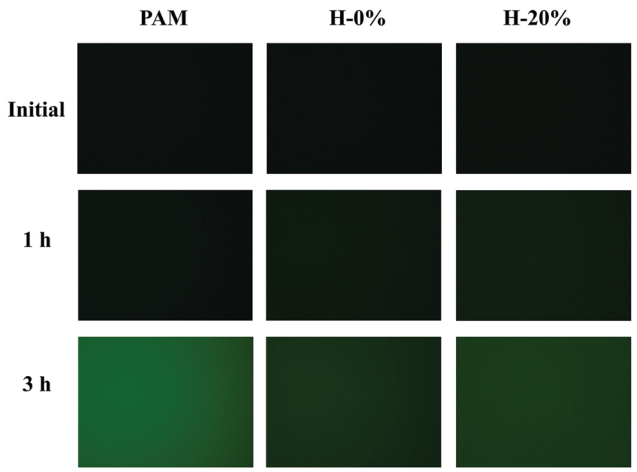

Fig. 8 Fluorescence microscopy images of the PAM hydrogel, PSBMA hydrogel (H-0%), and PSBMA emulsion hydrogel (H-20%) after 1 and 3 hours of BSA-FITC solution exposure.

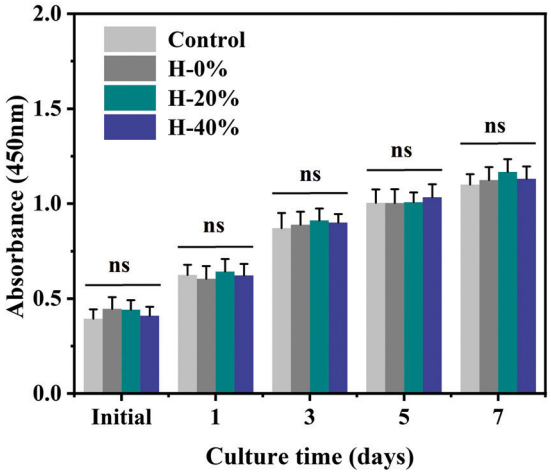

Fig. 10 Biocompatibility of the hydrogel and emulsion hydrogels measured by their effects on human fibroblast proliferation. (n = 6 per group; ns, no significance).

proliferation *in vitro*, making them suitable candidates for wound dressing with good biocompatibility.

Conclusions

In summary, we synthesized the thyme oil-loaded zwitterionic emulsion hydrogels by virtue of the CAA-stabilized O/W emulsion templates and the CAA-HRP-H_2O_2-initiated *in situ* polymerization of zwitterionic monomer (SBMA). The O/W emulsion droplets displayed good stability and uniform distribution. The corresponding lyophilized emulsion hydrogels exhibited a porous structure that was interconnected, regular, and homogeneous. By adjusting the amount of the inner phase, the zwitterionic emulsion hydrogels had outstanding and tunable mechanical properties. Furthermore, due to the excellent hydration performance, anti-fouling ability, antibacterial properties, and cyto-compatibility, as well as the enzyme-mediated polymerization process, the prepared thyme oil-loaded zwitterionic emulsion hydrogels might hold great promise as future antibacterial wound dressing materials in biomedical fields.

Conflicts of interest

There are no conflicts to declare.

Acknowledgements

This work was financially supported by the National Natural Science Foundation of China (Grant No. 21805031 and No. 81900604) and the Key Clinical Project of Peking University Third Hospital (BYSYZD2019038).

References

1 L.-H. Chen, L.-C. Cheng and P. S. Doyle, *Adv. Sci.*, 2020, **7**, 2001677.
2 O. Torres, B. Murray and A. Sarkar, *Trends Food Sci. Technol.*, 2016, **55**, 98–108.
3 T. Farjami and A. Madadlou, *Trends Food Sci. Technol.*, 2019, **86**, 85–94.
4 Y. Singh, J. G. Meher, K. Raval, F. A. Khan, M. Chaurasia, N. K. Jain and M. K. Chourasia, *J. Controlled Release*, 2017, **252**, 28–49.
5 S. M. Hashemnejad, A. Z. M. Badruddoza, B. Zarket, C. R. Castaneda and P. S. Doyle, *Nat. Commun.*, 2019, **10**, 2749.
6 J. Wang, Y. Li, Y. Gao, Z. Xie, M. Zhou, Y. He, H. Wu, W. Zhou, X. Dong, Z. Yang and Y. Hu, *Ind. Crops Prod.*, 2018, **112**, 281–289.
7 K. Ahmed, Y. Li, D. J. McClements and H. Xiao, *Food Chem.*, 2012, **132**, 799–807.
8 Y. S. Zhang and A. Khademhosseini, *Science*, 2017, **356**, eaaf3627.
9 J. Zhu, F. Li, X. Wang, J. Yu and D. Wu, *ACS Appl. Mater. Interfaces*, 2018, **10**, 13304–13316.
10 H. B. Eral, M. O'Mahony, R. Shaw, B. L. Trout, A. S. Myerson and P. S. Doyle, *Chem. Mater.*, 2014, **26**, 6213–6220.
11 A. Z. M. Badruddoza, P. D. Godfrin, A. S. Myerson, B. L. Trout and P. S. Doyle, *Adv. Healthcare Mater.*, 2016, **5**, 1960–1968.
12 X. Bao, Y. Yu, Q. Wang, P. Wang and J. Yuan, *ACS Sustainable Chem. Eng.*, 2019, **7**, 12973–12980.
13 F. Lee, K. H. Bae and M. Kurisawa, *Biomed. Mater.*, 2015, **11**, 014101.
14 M. D. Attieh, Y. Zhao, A. Elkak, A. Falcimaigne-Cordin and K. Haupt, *Angew. Chem., Int. Ed.*, 2017, **56**, 3339–3343.
15 T. Su, D. Zhang, Z. Tang, Q. Wu and Q. Wang, *Chem. Commun.*, 2013, **49**, 8033–8035.
16 L. Rong, X. Shen, B. Wang, Z. Mao, X. Feng and X. Sui, *Int. J. Biol. Macromol.*, 2020, **147**, 18–23.
17 V. Ryu, D. J. McClements, M. G. Corradini and L. McLandsborough, *Food Chem.*, 2018, **245**, 104–111.
18 J. Wu, C. He, H. He, C. Cheng, J. Zhu, Z. Xiao, H. Zhang, X. Li, J. Zheng and J. Xiao, *J. Mater. Chem. B*, 2017, **5**, 4595–4606.
19 H. He, Z. Xiao, Y. Zhou, A. Chen, X. Xuan, Y. Li, X. Guo, J. Zheng, J. Xiao and J. Wu, *J. Mater. Chem. B*, 2019, **7**, 1697–1707.
20 S. Jiang and Z. Cao, *Adv. Mater.*, 2010, **22**, 920–932.
21 L. Mi and S. Jiang, *Angew. Chem., Int. Ed.*, 2014, **53**, 1746–1754.
22 R. Lalani and L. Liu, *Biomacromolecules*, 2012, **13**, 1853–1863.
23 J. Wu, Z. Xiao, A. Chen, H. He, C. He, X. Shuai, X. Li, S. Chen, Y. Zhang, B. Ren, J. Zheng and J. Xiao, *Acta Biomater.*, 2018, **71**, 293–305.
24 Z. Wang, J. Chen, L. Wang, G. Gao, Y. Zhou, R. Wang, T. Xu, J. Yin and J. Fu, *J. Mater. Chem. B*, 2019, **7**, 24–29.
25 Z. Lei and P. Wu, *Nat. Commun.*, 2018, **9**, 1134.
26 B. Li, Z. Yuan, P. Zhang, A. Sinclair, P. Jain, K. Wu, C. Tsao, J. Xie, H.-C. Hung, X. Lin, T. Bai and S. Jiang, *Adv. Mater.*, 2018, **30**, 1705728.
27 A. Sinclair, M. B. O'Kelly, T. Bai, H.-C. Hung, P. Jain and S. Jiang, *Adv. Mater.*, 2018, **30**, 1803087.
28 H. Liu, X. Sui, H. Xu, L. Zhang, Y. Zhong and Z. Mao, *Macromol. Mater. Eng.*, 2016, **301**, 725–732.
29 Y. Liang, J. He and B. Guo, *ACS Nano*, 2021, **15**, 12687–12722.
30 K.-T. Huang, Y.-L. Fang, P.-S. Hsieh, C.-C. Li, N.-T. Dai and C.-J. Huang, *J. Mater. Chem. B*, 2016, **4**, 4206–4215.

